ELSEVIER

Marine Geology 170 (2000) 443–459

MARINE GEOLOGY
INTERNATIONAL JOURNAL OF MARINE GEOLOGY, GEOCHEMISTRY AND GEOPHYSICS

www.elsevier.nl/locate/margeo

In situ particle size spectra and density of particle aggregates in a dredging plume

O.A. Mikkelsen*, M. Pejrup

Institute of Geography, University of Copenhagen, Øster Voldgade 10, DK-1350 Copenhagen K, Denmark

Received 13 September 1999; accepted 31 July 2000

Abstract

An in situ laser particle sizer, the LISST-100, was used to describe the spatial variation of beam attenuation coefficient, in situ particle size spectra and aggregate densities in a dredging plume in the sound Øresund between Denmark and Sweden. The results proved that the above mentioned parameters varied significantly within the investigated length of the plume (approximately 2 km). It is shown how the small single primary particles aggregate and change the in situ particle size spectra into a slightly better sorted and coarser size distribution, and at the same time how the mean density of particles/aggregates decreases significantly. This shift in the state in which the particles exist in the water effectively changes the optical response of the mass of particles suspended in the water. It is shown that adequate correlations between mass concentrations and beam attenuation coefficients can only be obtained if parameters describing the in situ quality and state of the mass of particles, e.g. standard deviation of the size spectra and volume concentration, is included in the regression. From the spatial variation in mean density and in situ particle size, it was possible to calculate the spatial difference in settling velocity. It was found that the difference in settling velocity was only about a factor of 1.7, because increasing in situ particle size was counter-balanced by decreasing mean density. Furthermore, the time-scale of flocculation within the plume was found to be in the order of 50 min.

Keywords: Laser in situ scattering and transmissometry; Flocculation; Floc density; Grain-size analysis; Settling; Suspended sediment

1. Introduction

For decades, optical measurements with transmissometers or optical backscatter sensors (OBS) have been used to determine the mass concentration of suspended particulate matter in the open ocean, estuaries and rivers (e.g. Jones and Wills, 1956; Drake, 1974; Gibbs, 1974; McCave, 1983; Spinrad et al., 1983; Gardner et al., 1985; Riethmüller et al., 1988; Gippel, 1989; Jago and Jones, 1998).

It has been shown in laboratory experiments by, for example, Baker and Lavelle (1984), Conner and De Visser (1992), Gibbs and Wolanski (1992) and Benns and Pilgrim (1994) that the optical measurements are strongly dependent not only on the suspended sediment concentration (SSC) but also on the size distribution of the suspended sediment. For example, Baker and Lavelle (1984) showed that the variation in (disaggregated) grain-size distribution at a fixed SSC caused a 14-fold variation in the beam attenuation coefficient (c) from a transmissometer, c increasing with decreasing mean grain-size.

* Corresponding author. Tel.: +45-35-32-25-00; fax: +45-35-32-25-01.

E-mail addresses: oam@geogr.ku.dk (O.A. Mikkelsen), mp@geogr.ku.dk (M. Pejrup).

0025-3227/00/$ - see front matter
PII: S0025-3227(00)00105-5

Nomenclature

c	Beam attenuation coefficient, m^{-1}
$c(670)$	Beam attenuation coefficient at 670 nm, m^{-1}
SSC	Suspended sediment concentration, mg/l.
VC	Volume concentration, μl/l
ND	Normalised effective density, normalised with the highest effective density
W_s	Settling velocity
d	Particle diameter (in Stokes Law)
g	Acceleration due to gravity, m/s^2
ρ_F	Floc bulk density, kg/m^3
ρ_W	Density of sea water, kg/m^3
$(\rho_F - \rho_W)$	Effective density, kg/m^3
τ	Optical transmission, dimensionless.
$\bar{x}$	In situ mean grain-size, Φ or μm
$\bar{x}_p$	Mean grain-size of the primary particles, Φ or μm
σ	In situ standard deviation of the grain-size spectra, Φ
σ_p	Standard deviation of the primary particle size spectra, Φ
μ	Molecular viscosity, kg/ms
r	Correlation coefficient in regression analysis
b	*Y*-intercept in correlation equation
n	Number of samples used for averaging or in regression analysis
d.f.	Degrees of freedom

Fine-grained sediments are known to flocculate in sea-water and thereby alter their size-distribution towards a more coarse-grained one (e.g. Kranck, 1975, 1981; Pejrup, 1988; Eisma, 1993; Mikkelsen and Pejrup, 1998). The flocculation process also causes a decrease in the density of the suspended aggregates when their size increases (e.g. Gibbs, 1985; Fennessy et al., 1994; Ten Brinke, 1994). Consequently, the flocculation process greatly affects the optical measurements.

This poses some problems when using, for example, a transmissometer for long-term monitoring and one subsequently attempts to correlate the observed beam attenuation coefficients with measured values of SSC obtained, e.g. during a few intensive field periods. In this case there may be a large uncertainty with respect to the effect of flocculation and/or size spectra of the suspended matter on the determination of c in the intervening periods between field sampling periods. This may explain why some workers (e.g. Wells and Kim, 1991; Jago and Jones, 1998) have reported poor correlation coefficients between their measurements of c and SSC.

There is a need to measure, simultaneously, values of c, SSC, volume concentration (VC) and in situ particle size spectra of the suspended sediment (i.e. floc-size), in order to incorporate the effect of a changing in situ grain-size and/or VC on c. This was attempted by Campbell and Spinrad (1987), who showed that c was correlated with VC, aggregate size and aggregate density. Their analyses of aggregate size were based on measurements with a Coulter Counter. However, as a Coulter Counter has been shown by Gibbs (1982) to destroy flocs having a diameter larger than 7–25% of the diameter of the orifice used, the Coulter Counter does not describe in situ aggregate size adequately. Therefore, an instrument that does not disrupt the fragile aggregates is required.

Such an instrument is the LISST-100 in situ laser diffraction analyser, manufactured by Sequoia Scientific, Inc., USA. The LISST (Laser In Situ Scattering and Transmissometry) uses the laser diffraction principle (see, e.g. Agrawal et al., 1991), known from laboratory lasers like Malvern or Fritsch, to determine the size of suspended particles. However, it is

designed to be submerged to a depth of maximum 300 m and equipped with a built-in datalogger.

With the advent of the LISST-100, it has become possible to measure simultaneously values of c, VC and in situ particle size spectra in a close to non-intrusive manner. It should be noted, that laser diffraction measurements has been used to measure and characterise suspended sediments and floc-sizes in situ since 1985 (see, e.g. Bale and Morris, 1987; McCabe et al., 1993; Agrawal and Pottsmith, 1994; Gentien et al., 1995; Bale, 1996; van der Lee, 1998). Also, several authors have used laser diffraction measurements to measure floc-size distribution in the laboratory (e.g. Biggs and Lant, 2000; Van Leussen, 1994; Lick et al., 1993; Tsai et al., 1987). The LISST-100 however, is the first in situ laser that measures c, VC and in situ particle size spectra.

In the present study, a LISST-100 was used for profiling in a lime ($CaCO_3$) dredging plume. Water samples were taken simultaneously with LISST-100 measurements. It is shown how the particles flocculate over a relatively short time and distance and how it is possible to use the LISST-100 to calculate the effective mean density of the particles in suspension. Furthermore, multiple linear regressions were carried out between c and SSC, VC, $\bar{x}$, σ and the normalised effective mean density (ND). It is shown how the correlation coefficient increases significantly when parameters describing the state of the suspended particles is included for description of the variation in c. Additionally it is shown that as the lime particles flocculate and their size increases, their mean density decreases correspondingly, so that the computed difference in settling velocity between the investigated profiles only is in the order of a factor of 1.7. This is in accordance with previous investigations of settling velocities in similar dredging plumes in the area (Edelvang, 1998). Finally, an estimate of the time-scale of flocculation is calculated and found to be within the order of 50 min. This is in good agreement with recent model results (Winterwerp, 1999).

2. Methods

On 2nd September 1998 a LISST-100 was deployed at four positions (denoted I, II, III and IV) in a dredging plume in the sound Øresund, between Denmark and Sweden (Fig. 1). The four positions were all within the plume and at an increasing distance from the dredger. At each position, one vertical profile was made from surface to bottom. When profiling, the research vessel drifted freely with the current within the plume. The water depth was approximately 9 m.

The LISST-100 measured the particle size distribution in 32 logarithmically spaced size classes in the range 1.25–250 μm (a LISST-100 type B). Sampling was carried out at a frequency of 2.2 Hz. Every two samples were averaged and the average stored, thus yielding a data frequency of 1.1 Hz, or 67 samples per minute. This was done in order to carry out some sort of averaging with respect to small number statistics regarding the coarse-grained fraction of the size distribution.

Also, while profiling, 2-l water samples for determination of SSC were taken at 2, 4 and 6 m below the surface (mbs). The samples were taken with a vertical cylindric sampler, effectively cutting out a vertical cylinder of water. The height of the sampler is 40 cm, and a sample taken, e.g. 2 mbs thus contains water and suspended sediment from the interval 1.8–2.2 mbs. Salinity was measured in the laboratory. The water samples were suction-filtered on pre-weighed Millipore filters, type HA (CEM filters), with a nominal retention diameter of 0.45 μm. The filters were oven-dried at 65°C for one and a half hours, allowed to cool for half an hour and then weighed with an accuracy of 0.2 mg. Blanks were used to correct for changes in humidity.

In order to analyse the grain-size distribution of the primary particles, the sediment on the filters was dispersed in a solution of 0.01 M $Na_4P_2O_7$ and sonified for two minutes in a Branson Sonifier 250. The dispersed sediment was then analysed in a laser diffraction analyser, a Malvern MasterSizer/E. The Malvern was equipped with a 100 mm lens, capable of analysing grain-sizes in the range of 0.5–180 μm.

A detailed description of the design and the operational principles of the LISST-100 can be found in Agrawal and Pottsmith (1994), Agrawal et al. (1996) or Traykovski et al. (1999). However, the basic principles will be explained very briefly here.

The LISST-100 measures the angular distribution of forward scattered light energy over a path length of 5 cm, using a collimated laser beam with a wavelength

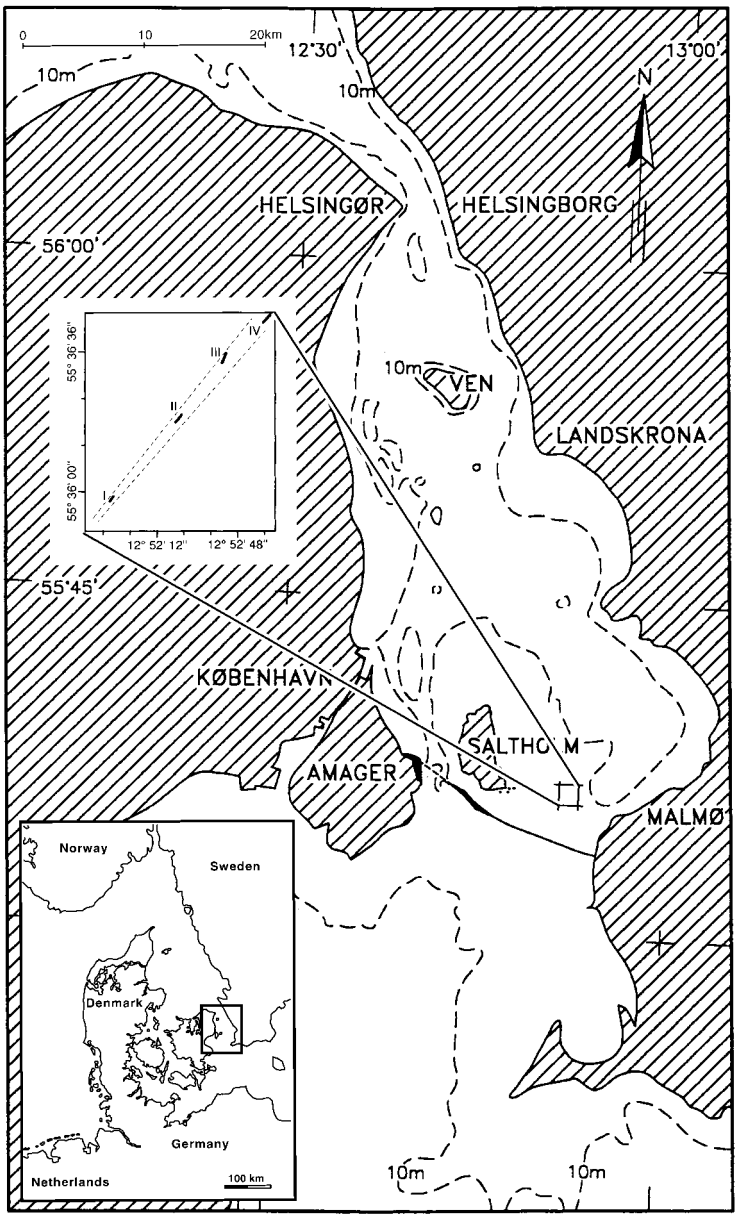

Fig. 1. Map of the Øresund area between Denmark and Sweden. Inset shows the position of the profiles (I–IV) in the investigated dredging plume. The position of the dredger was approximately 300 m SW of profile I. The edges of the plume are indicated by the dashed lines.

of 670 nm. The energy of the scattered light is detected on 32 logarithmically spaced ring detectors and stored in a built-in datalogger. When data collection is complete, these raw data are offloaded and mathematically inverted. The inversion yields the area distribution of the suspended particles (in 32 size classes). By multiplying the area distribution by the diameter of each size class, the particle volume distribution is obtained. Summing the volume distributions in all 32 size classes and dividing by an instrument-dependent calibration constant, the absolute VC (μl/l), is found. The part of the light not scattered is

Fig. 2. Photograph of a typical dredging plume in the Øresund. Current direction is towards the North (bottom of photograph). Note the sharply demarcated edges of the plume. (Photo by Poul Hammer, Danish Hydraulic Institute.)

detected by a photo-diode in the centre of the ring detector, thus yielding the optical transmission, τ, of the water. From the optical transmission the beam attenuation coefficient, $c(670)$, can be calculated using Eq. (1)

$$c(670)\ (\mathrm{m}^{-1}) = -\frac{1}{0.05\ \mathrm{m}} \times \ln(\tau) \quad (1)$$

The processed data output from the LISST-100 thus consists of a particle volume distribution (in 32 size classes), an absolute VC (in μl/l) and a beam attenuation coefficient at 670 nm (in m^{-1}). Furthermore, the LISST-100 records the temperature and pressure. From the particle volume distribution, statistical parameters such as $\bar{x}$ and σ can then be calculated.

All software necessary for obtaining and analysing raw data is supplied by the manufacturer of the LISST-100, Sequoia Scientific Inc., USA. Regarding the data in this paper, the raw scattering data were analysed using version 3.20 of the LISST-100 data analysis program (released March 1998). Subsequent calculation of $\bar{x}$, σ and other statistical parameters were carried out using a spreadsheet.

3. Results and discussion

The approximate extension of the investigated part of the plume and the positions of the profiles appears from Fig. 1. Profile IV is the profile farthest away from the dredger (not shown), while profile I is the profile closest to the dredger. The dredger was working approximately 300 m SW of the beginning of profile I.

Within the plume, the salinity was constant 7.6 at all positions. The sea surface was flat and the wind was calm throughout the measuring period.

Fig. 2 is a photograph of a typical dredging plume (which appears white) in the Øresund. The edges of the plume are seen very clearly and there is a very sharp demarcation between the plume and the surrounding waters. When sailing within a plume, this demarcation also appears very clearly. It is usually possible to detect whether or not one is positioned within the plume with an accuracy of one or two metres.

3.1. Particle size spectra

3.1.1. In situ spectra

The in situ grain-size spectra in profile III and IV are seen to be almost identical (Fig. 3), so are the spectra from profile II and I. The size spectra in profile II and I (closest to the dredger) are in fact bimodal, with modes around 2.9 and 4.1 Φ (135 and 58 μm), respectively. The size spectra in profiles III and IV are unimodal, with a mode around 2.6 Φ (165 μm). Almost no particles finer than approximately 4 Φ (64 μm) are seen in profiles III and IV, whereas there is an abundance of particles finer than 4 Φ in profile I and II. The amount of particles finer than approximately 3.5 Φ (90 μm) increases slightly from profile III to IV. There is also a slight tendency for the concentration of particles about 2.5 Φ (175 μm) to increase towards the bottom in profile IV. This could indicate that settling of some of the coarser particles took place between profile III and IV. The spectra in Fig. 3 were created by averaging the spectra obtained around the specific depth ±0.2 m in

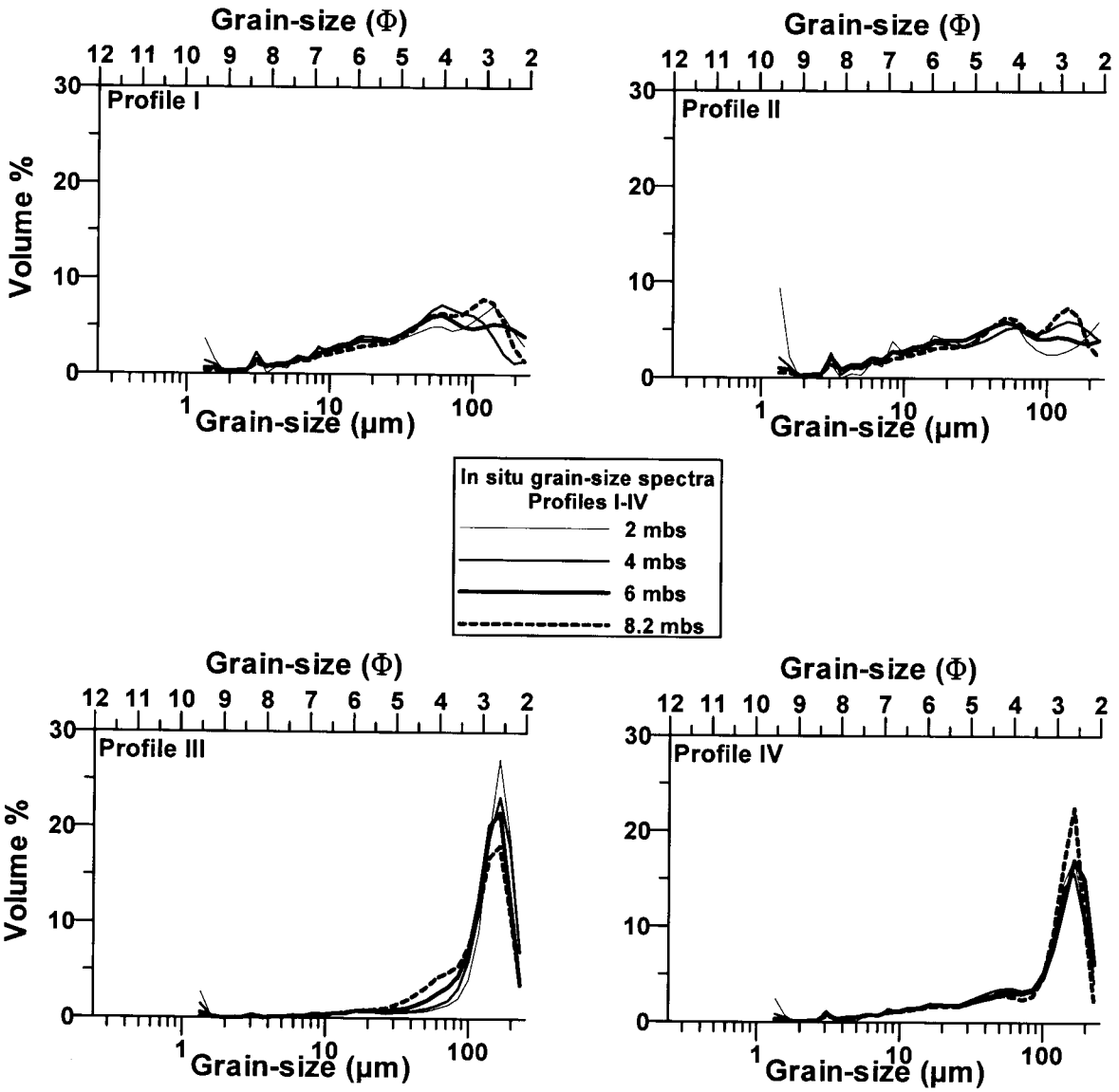

Fig. 3. In situ grain-size spectra at 2, 4, 6 and 8.2 mbs in the four profiles. Note the disappearance of particles smaller than 4 Φ (64 mm) in profile III and IV compared to profile I and II.

order to compare with the water samples obtained with the vertical cylindric sampler, which include water from ±0.2 m of the depth where the sample was taken (cf. Section 2).

When profiling, the research vessel drifted freely with the current within the plume. Due to the velocity gradient, the current velocity at the surface would be higher than closer to the bottom. Consequently, there has been a small, but steady flow of water through the optics end of the LISST-100.

Two distinct features of the spectra in Fig. 3 appears: A peak around 8.3 Φ (3 μm) is seen in all spectra, so is a "tail" at the very fine-grained end of the spectra. These features are by far most pronounced in profile I and II. The rising tails are a result of the way the software handles the scattering pattern

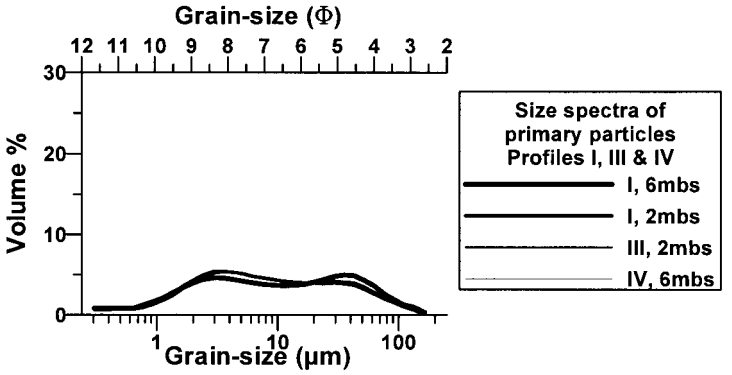

Fig. 4. Selected grain-size spectra of the primary particles in the profiles. Note the similarity of the spectra, when compared to the large difference in the in situ spectra in Fig. 2.

resulting from particles smaller than the lower size range of the instrument. It is an artifact and the distributions do not really show this rising tail. The peaks around 8.3 Φ are most likely due to a minor error in the software handling the raw scattering data (Y.C. Agrawal, Sequoia Scientific, Inc., personal communication). The LISST-100 in general shows good agreement with single-sized standard particles (e.g. polystyrene spheres), and it has been shown by Traykovski et al. (1999), that it also shows good agreement with natural, sieved sediments.

It is clear, that if the peaks (at 8.3 Φ) and tails (at 9.4 Φ) are not related to the actual size-distribution, the calculation of $\bar{x}$, σ and VC will be slightly incorrect. This has been tested by calculating $\bar{x}$, σ and VC, assuming a volume percentage of 0 in the 8.3 and 9.4 Φ size-classes. It was found that the change in $\bar{x}$, and σ in general was less than one size-class (0.24 Φ). With respect to the change in VC it was found that the largest decrease was 5.7% with an average of 3.2%. Such small changes are considered negligible and no attempts have been made to carry out any sort of manual adjustment of the data. Only for profile II, 2 mbs was the difference in mean grain-size larger than one size-class when calculated with and without the tail. Consequently all size spectra from 0–3.8 mbs in profile II will not be considered further in this paper.

3.1.2. Primary particle size spectra

Fig. 4 shows selected size spectra of the primary particles of the suspended sediment. Clearly, the size spectra of the primary particles do not show the same variation as the in situ spectra in Fig. 3.

The spectra are seen to be bi-modal, with modes at approximately 5.0 and 8.3 Φ (36 and 3 μm, respectively). The mean grain-size of the primary particles ($\bar{x}_p$) varies between 6.7 and 6.9 Φ (10–8 μm), with a standard deviation (σ_p) varying between 1.9 and 2.0 Φ.

As dredging operations create a significant amount of turbulence in the waters surrounding the dredger, one could speculate that the particles showing up as finer than 4 Φ (64 μm) in Fig. 3 were in fact air-bubbles, released by the dredging process. In fact, it has been shown that the LISST-100 is able to detect and measure the diameter of bubbles in water (Observations of Bubbles in the Laboratory Using the LISST-100, Application Note L003, Sequoia Scientific, Inc.). Thus it is satisfying that the grain-size spectra of the primary particles show that primary particles finer than 4 Φ in fact do exist in the water. This shows, that at the very least, the particles finer than 4 Φ in Fig. 3 do not relate solely to air bubbles. This is even more evident, as there is a large similarity between the spectra from different depths within profiles I and II. If bubbles were a major cause of the particles showing up as finer than 4 Φ in profiles I and II in Fig. 3, one would expect the percentage of these particles to increase towards the surface (as the bubbles would tend to rise towards the surface).

It is also important to realise that because the primary particle size spectra in Fig. 4 do not show any variation with depth or between profiles, the

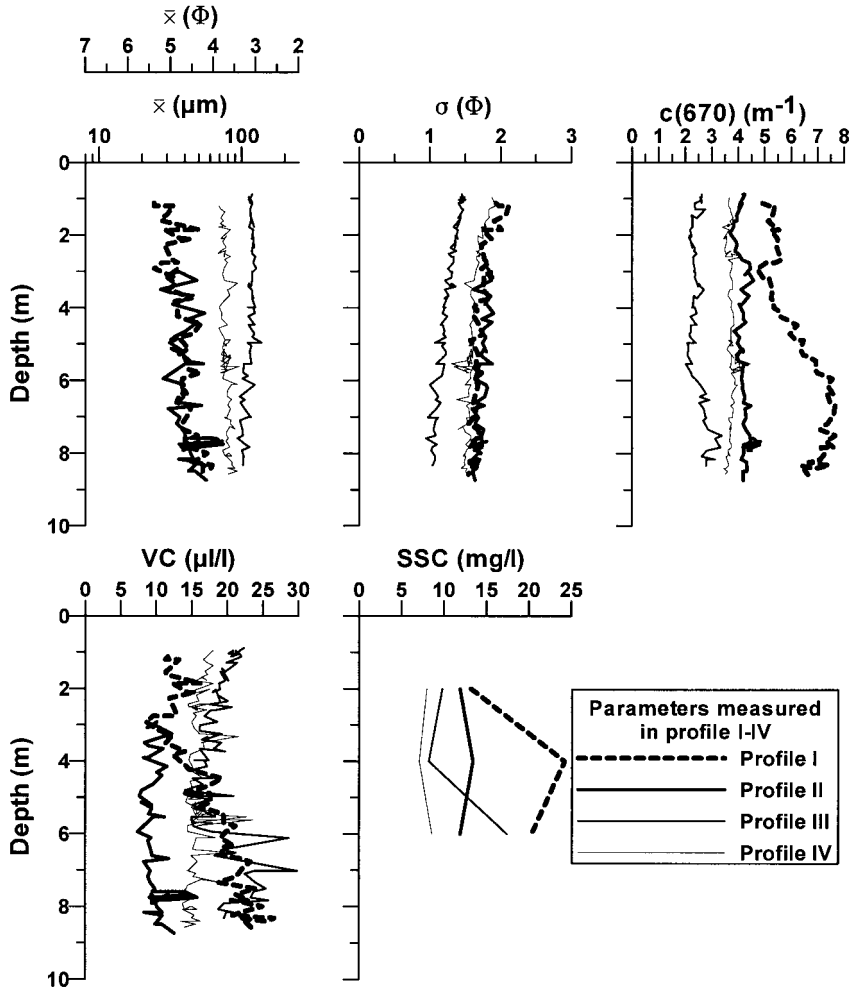

Fig. 5. The depth variation of $\bar{x}$, σ, c(670), VC and SSC in the four profiles.

Table 1
Depth integrated values ± one standard deviation of the parameters measured in the profiles (cf. Fig. 5); $\bar{x}$, mean grain-size; σ, standard deviation; c(670), beam attenuation coefficient; VC, volume concentration; SSC, suspended sediment concentration; n, number of LISST-100 measurements averaged to calculate $\bar{x}$, σ, c(670) and VC; mean values of SSC calculated by averaging the three samples from each profile

	Profile I	Profile II	Profile III	Profile IV
$\bar{x}$ (Φ)	4.7 ± 0.3	4.6 ± 0.3	3.2 ± 0.2	3.7 ± 0.1
$\bar{x}$ (µm)	39 (31–47)	41 (34–51)	109 (95–125)	77 (72–83)
σ (Φ)	1.7 ± 0.1	1.7 ± 0.1	1.4 ± 0.3	1.7 ± 0.2
c(670) (m^{-1})	6.3 ± 1.0	4.3 ± 0.2	2.6 ± 0.3	3.8 ± 0.2
VC (µl/l)	17.0 ± 4.8	10.1 ± 1.7	19.5 ± 2.9	16.8 ± 2.0
SSC (mg/l)	19.2 ± 5.6	12.4 ± 0.9	11.8 ± 4.9	7.9 ± 0.8
n	55	51	108	165

Table 2
Calculation of depth averaged aggregate density in profile I–IV; SSC and VC are mean values ± one standard deviation; $\rho_F - \rho_W$, effective density; ρ_F, floc bulk density; ND, normalised effective density; ND is calculated as follows: $(\rho_F - \rho_W)/1283$; note that effective density in mg/ml is the same as kg/m^3

	Profile I	Profile II	Profile III	Profile IV
Mean SSC (mg/l)	19.2 ± 5.6	12.7 ± 0.8	11.8 ± 4.9	7.9 ± 0.8
Mean VC (μl/l)	16.9 ± 1.6	9.9 ± 1.3	17.2 ± 1.7	16.1 ± 1.8
$\rho_F - \rho_W$ (mg/ml)	1136	1283	686	491
ρ_F (kg/m^3)	2146	2293	1696	1501
ND	0.89	1.00	0.53	0.38

changes in the in situ size spectra seen in Fig. 3 cannot be related to single grains settling out of suspension. If the removal of particles finer than 4 Φ (64 μm) in Fig. 3 (profile I and II) were to be related to single grain settling, then these particles should also be missing in Fig. 4. This is not the case.

3.2. General observations

In Fig. 5, the vertical variation of $\bar{x}$, σ, $c(670)$, VC and SSC in the four profiles is shown. Average values of these parameters ± one standard devation are shown in Table 1.

From Fig. 5 and Table 1 it appears that $\bar{x}$ in profile III and IV is very constant throughout the water column, about 3.2 (109 μm) and 3.7 Φ (77 μm), respectively. However, $\bar{x}$ in profile I and II is seen to be generally finer than in profile III and IV and coarsening towards the bottom, from approximately 5.4 Φ (24 μm) at the top to 4 Φ (64 μm) at the bottom. In profile I, II and IV there is a general decrease in σ from 1.9 Φ at the surface to 1.5 Φ at the bottom. In profile III σ is smaller, but it also decreases from top to bottom. The sorting in profile III thus is somewhat better than in the rest of the profiles.

With respect to $c(670)$, almost no vertical variation is seen except in profile I. In this profile $c(670)$ increases from 5 m^{-1} at the surface to 7.5 m^{-1} close to the bottom. A general decrease in $c(670)$ from profile I to IV is also seen from Fig. 5 and Table 1.

The VC in profile III and IV is almost identical to a depth of 6 mbs. The VC in profile III then increases towards the bottom. This is somewhat in accordance with the concurrent increase in SSC in profile III. In profile II, VC is almost constant throughout the water column, whereas in profile I, VC increases steadily from 3 mbs towards the bottom.

A general decrease in SSC is seen from profile I to IV. In profile II and IV almost no vertical variation is found, whereas there is a much larger vertical variation in profile I and III. Note that the large value of SSC at 4 mbs in profile I does not result in a corresponding increase in $c(670)$ at 4 mbs. This could be an effect of changing particle characteristics or a result of the variation in time and space between the LISST measurement and the sampling of water (1–2 m in space laterally and up to 40 s temporally).

3.3. Calculating particle density with LISST-100

When water samples for determination of SSC are taken simultaneously with a LISST-100 measurement of VC, it is possible to calculate the effective mean density of the suspended particles ($\rho_F - \rho_W$), where ρ_F is the floc bulk density and ρ_W is the density of the water, Eq. (2)

$$(\rho_F - \rho_W) = \frac{SSC}{VC} \quad (2)$$

The density of the seawater was 1010 kg/m^3, and ρ_F can then be calculated. In Table 2 appears the mean SSC at the depths 2–6 mbs for the profiles I–IV, mean VC in μl/l, effective density in mg/ml (= kg/m^3), floc bulk density in kg/m^3 and the normalised effective mean density (ND), normalised with the highest effective density from Table 2, 1283 kg/m^3.

The normalised effective mean density was then calculated and tabulated together with SSC, $c(670)$,

Table 3
Average values at 2, 4, 6 and 8.2 mbs in the profiles; calculated average values of $c(670)$, $\bar{x}$, σ, VC and ND at the depths 2, 4, 6 and 8.2 mbs ±0.2 m together with the SSC at 2, 4 and 6 mbs; around each depth, n LISST-100 measurements were averaged

Profile no	Depth (mbs)	SSC (mg/1)	$c(670)$ (m^{-1})	$\bar{x}$ (Φ)	σ (Φ)	VC (μ1/1)	ND	n
I	2	13.2	5.44	4.69	1.87	14.61	0.51	4
I	4	24.2	5.45	4.86	1.65	13.53	1.00	4
I	6	20.3	7.31	4.59	1.68	20.02	0.57	3
I	8.2	–	6.96	4.23	1.64	23.62	–	6
II	2	11.9	3.80	–	–	–	–	4
II	4	13.4	4.12	4.68	1.83	9.50	0.79	3
II	6	11.9	4.15	4.86	1.75	8.49	0.78	3
II	8.2	–	4.20	4.53	1.67	10.02	–	4
III	2	9.8	2.18	3.07	1.36	18.52	0.30	4
III	4	8.2	2.33	3.07	1.21	16.62	0.28	5
III	6	17.4	2.36	3.20	1.11	19.49	0.50	4
III	8.2	–	2.87	3.28	1.03	20.78	–	6
IV	2	8.0	3.54	3.72	1.72	16.40	0.27	5
IV	4	7.1	3.77	3.80	1.62	14.86	0.27	3
IV	6	8.6	3.87	3.63	1.56	15.72	0.31	4
IV	8.2	–	3.62	3.62	1.49	14.80	–	6

$\bar{x}$, σ and VC for all depths where water samples were taken in the four profiles (Table 3).

From the normalised densities in Tables 2 and 3 it is seen that the effective mean density have similar large values in profiles I and II, i.e. the two profiles nearest the dredger. Furthermore, it is seen that in profiles III and IV, farthest away from the dredger, the effective mean density in general decreases to 40–50% of the value in profiles I and II.

The decrease in effective mean density might theoretically be explained by a large algae/sediment ratio, as algae has a density lower than inorganic sediment (in this case, lime). In fact, algae do dominate the suspended particulates in the "background waters" in the summer (Edelvang, 1998). However, it is seen from Table 3 that the mean SSC 2–6 mbs was 8 mg/l in profile IV, which is approximately a factor of 4–8 larger than the normal background concentration in Øresund of 1–2 mg/l (Edelvang, 1998). Therefore, the algae/sediment ratio in profile I–IV probably has been much lower than in the water outside the plume. Consequently it is not likely that the decrease in effective mean density is related to increased algae concentration from profile I to profile IV.

As it can be seen from Fig. 5 and Table 1 that $\bar{x}$ in general increases from profile I to profile IV, the relative decrease in mean density seen from Table 2 can therefore be explained by flocculation. It should be acknowledged that the open-ended size spectra in Fig. 3 means that not all the volume of the suspended sediment is detected by the LISST. This uncertainty, however, is considered insignificant when compared to the uncertainty there is in calculating density from the mean VC and SSC. The density calculated in this manner should probably be used as a qualitative indicator on changes in density, not so much as an accurate measure of the particle density.

In Fig. 6, the effective mean density in profiles I–IV is plotted against $\bar{x}$ and it can be seen that the effective mean density decreases from 1411 kg/m^3 in profile II to 478 kg/m^3 in profile IV, while $\bar{x}$ increases from 4.7 (39 μm) to 3.7 Φ (77 μm). The effective density in profile I and II is seen to vary between 900 and 1400 kg/m^3. This is somewhat in contrast with what have been reported by other workers using state-of-the-art video systems (e.g. Ten Brinke, 1994; Fennessy et al., 1994), who found the maximum effective density to lie in the range of approximately 500 and 900 kg/m^3, respectively.

This discrepancy, however, is most likely related to

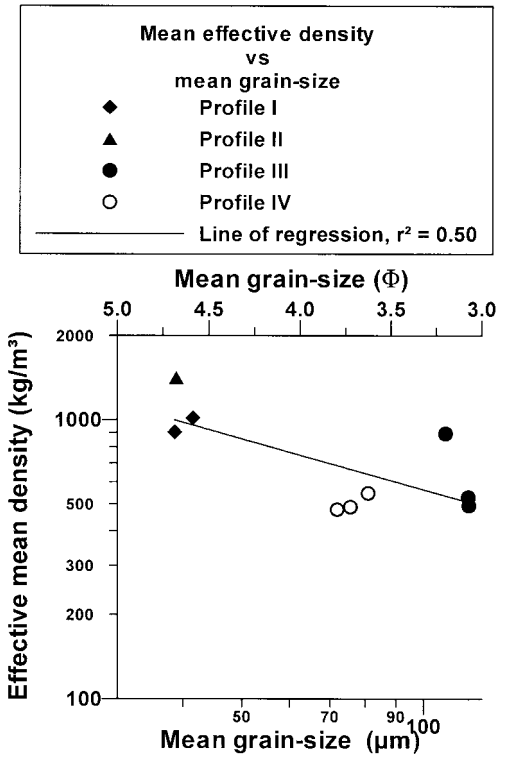

Fig. 6. Plot of effective density versus in situ particle size in the four profiles. The effective mean density is generally seen to decrease with: (1) increasing mean grain-size, and (2) from profile I/II to III/IV.

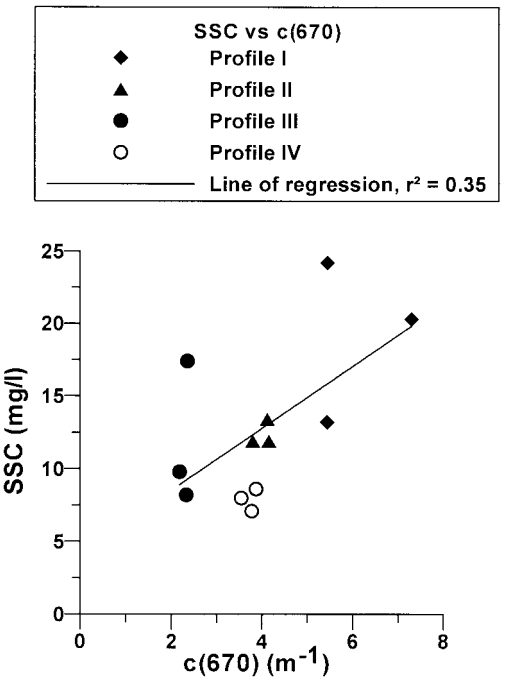

Fig. 7. Scatterplot showing the correlation between SSC and $c(670)$ for the water samples taken in the profiles. Almost no correlation between SSC and $c(670)$ is seen.

the fact that the LISST-100 also detects the single mineral grains that are not part of any aggregates. The video systems used by Ten Brinke (1994) and Fennessy et al. (1994) have a lower limit of resolution of 50 and 20 μm, respectively, meaning that these systems are almost exclusively capable of analysing aggregates and not single mineral grains or the smallest flocs. The lower limit of resolution of a type B LISST-100 is 1.25 μm, meaning that the instrument is capable also of measuring small sediment flocs and single mineral grains. Consequently, as not all of the particles measured by the LISST are aggregates, one should not expect the effective density calculated to lie within the range reported by Ten Brinke (1994) and Fennessy et al. (1994). Because the instrument also detects single mineral grains (in this case $CaCO_3$) with a density of 2710 kg/m^3, much larger than the density of the aggregates, then the effective density calculated should be somewhat higher than the values reported using video systems, capable mainly of measuring aggregates.

3.4. The dependence of c(670) on the measured variables

For decades, the output from transmissometers or OBS's has been used to calculate the SSC. This calculation has usually been carried out in form of a linear regression analysis between measured values of the output from a transmissometer or an OBS and the corresponding SSC; the latter usually being obtained by filtering water samples taken simultaneously with the light measurement (e.g. Gippel, 1989). As mentioned earlier, this analysis quite often shows a good correlation, in the field as well as in the laboratory (e.g. Baker and Lavelle, 1984; Riethmüller et al., 1988; Gippel, 1989; Amos et al., 1992; Gibbs and Wolanski, 1992; Benns and Pilgrim, 1994), but as can be seen from Fig. 7, the observed correlation between $c(670)$ and SSC in the four profiles is insignificant.

Table 4
Results of the (multiple) linear regression analysis: b = intercept; r^2 = explanation of variance, d.f. = degrees of freedom in each regression analysis; example: in analysis no. 20, $c(670)$ (m^{-1}) = 0.22*SSC + 2.79*$\bar{x}$ − 7.14*ND − 6.44, r^2 = 0.95; the data sets in Table 3 were used in the regression analysis

Analysis No.	No. of independent variables	d.f.	SSC (mg/l)	$\bar{x}$ (Φ)	σ (Φ)	VC (μl/l)	ND	b	r^2
1	1	9	0.17	–	–	–	–	1.91	0.35
2	1	9	–	1.70	–	–	–	−2.80	0.65
3	1	9	–	–	4.28	–	–	−2.72	0.46
4	1	9	–	–	–	−0.04	–	4.61	0.008
5	1	9	–	–	–	–	2.99	2.53	0.24
6	2	8	0.07	1.44	–	–	–	−2.59	0.68
7	2	8	0.15	–	4.02	–	–	−4.26	0.75
8	2	8	0.17	–	–	−0.06	–	2.75	0.37
9	2	8	0.15	–	–	–	0.55	1.89	0.35
10	2	8	–	1.63	0.26	–	–	−2.92	0.65
11	2	8	–	2.60	–	0.28	–	−10.73	0.92
12	2	8	–	2.39	–	–	−2.46	−4.30	0.71
13	2	8	–	–	6.04	0.20	–	−8.52	0.61
14	2	8	–	–	3.62	–	1.62	−2.49	0.52
15	2	8	–	–	–	0.12	3.97	0.23	0.30
16	3	7	0.17	−0.25	4.60	–	–	−4.39	0.76
17	3	7	0.14	–	5.45	0.16	–	−8.78	0.85
18	3	7	1.27	–	–	−1.34	−29.45	22.95	0.61
19	3	7	−0.07	3.08	–	0.35	–	−12.82	0.95
20	3	7	0.22	2.79	–	–	−7.14	−6.44	0.95
21	3	7	0.28	–	5.32	–	−3.69	−6.07	0.86
22	3	7	–	2.28	1.25	0.29	–	−11.57	0.94
23	3	7	–	3.03	–	0.27	−1.71	−11.40	0.95
24	3	7	–	4.72	−4.92	–	−5.91	−4.13	0.78
25	3	7	–	–	5.69	0.32	3.47	−11.59	0.83
26	4	6	−0.10	3.60	−1.09	0.38	–	−13.14	0.95
27	4	6	0.60	–	4.69	−0.41	−12.29	1.27	0.88
28	4	6	0.13	2.90	–	0.12	−4.83	−8.58	0.96
29	4	6	0.22	3.07	−0.61	–	−7.41	−6.35	0.95
30	4	6	–	3.51	−1.08	0.26	−2.51	−10.98	0.96
31	5	5	0.08	3.34	−0.88	0.16	−4.33	−9.28	0.96

This could be related to the effect of grain-size on the beam attenuation coefficient and in order to try to determine this effect, linear regression analysis between $c(670)$ and the following independent variables were carried out: SSC (in mg/l), $\bar{x}$ (in Φ-units), σ (in Φ-units), VC (in μl/l) and ND. These variables are the ones with which c is considered dependent in the following, the reason being as follows.

For a given particle population, SSC and VC per se attenuate the light in a linear manner (Baker and Lavelle, 1984). To act physically correct, the signs of the constants associated with SSC and VC thus should be positive.

The in situ mean grain-size is important, because at a given concentration, fine-grained particles attenuate light more than coarser-grained particles. This is due to the larger specific surface area for fine-grained particles, compared to the coarser-grained ones. As $\bar{x}$ in this study is expressed in Φ-units, the sign of the constant associated with $\bar{x}$ should be positive. Then decreasing $\bar{x}$ (increasing Φ) will cause an increase in c.

With respect to the standard deviation, this probably

Table 5
Correlation matrix

	SSC	VC	ND	$\bar{x}$	σ
SSC	1				
VC	0.08	1			
ND	0.77	−0.57	1		
$\bar{x}$	0.53	−0.62	0.8	1	
σ	0.08	−0.59	0.4	0.83	1

also would have some influence on the beam attenuation coefficient. However, the sign of the constant associated with σ is not clear in advance; it probably is somewhat dependent on $\bar{x}$ and the size of σ itself. For example, at a constant value of SSC, consider a fine-grained size distribution. This will per se yield a (relatively) high value of c. This value of c is most likely to be affected by σ in such a way that if σ is small, it will accentuate the effect of the size distribution itself and consequently the effect on c will be positive, yielding a positive sign. On the other hand, if σ of this size-distribution is large, coarse particles will co-exist with the fine-grained sediment. As the effect of coarse particles (in general) is to lower c, then this could mean that the effect of the constant associated with σ was to lower c, yielding a negative sign.

The final independent variable, the normalised density, is supposed to affect the value of c in such a way that an increasing density "clears" the water, thus decreasing c. In order to act physically correct, the sign of the constant associated with ND thus should be negative.

A conceptual, empirical formula can thus be outlined.

$$c(670)\ (\mathrm{m}^{-1}) = k1 \times \mathrm{SSC}\ (\mathrm{mg/l}) + k2 \times \mathrm{VC}\ (\mu\mathrm{l/l}) + k3 \times \bar{x}\ (\Phi) \pm k4 \times \sigma\ (\Phi) - k5 \times \mathrm{ND} \pm k6 \quad (3)$$

To complete the list of variables affecting c, there should be added some sort of biological factors present in the water, e.g. algae concentration or algae species. However, it has not been possible to include these factors in the analysis, as no samples were taken for determination of concentration or species of algae present. But as discussed in Section 3.3, the impact of algae within the plume can most likely be considered negligible.

A multiple linear regression analysis between c and the five independent variables considered above was subsequently carried out. In each analysis, the data set resulting from the LISST profiles were used (Table 3). The resulting size and sign of the constants associated with the independent variables are shown in Table 4.

According to the previous argument pertaining to the sign of the constants, it is seen that the following analysis yields physically incorrect signs (the numbers corresponds to the analysis number in Table 4): 4, 5, 8, 9, 14, 15, 16, 18, 19, 25, 26, 27.

Furthermore, the remaining regressions must all fulfill the following criteria:

1. all the independent variables should be uncorrelated;
2. all the independent variables in each analysis should be of importance for the prediction of $c(670)$;
3. in each analysis, the correlation between $c(670)$ and the independent variables should be significant.

In Table 5 is found the correlation coefficients between the five variables used in the regression analysis.

By using a two-tailed test of correlation ($\alpha = 0.05$) with nine degrees of freedom, it was determined that the correlation between the independent variables could be considered significant only when the absolute correlation coefficient ($|r|$) was greater than 0.602. To determine if the independent variables were in fact important for the prediction of $c(670)$, a t-test ($\alpha = 0.05$) was used. Finally an F-test ($\alpha = 0.05$) was used to determine if the correlation between $c(670)$ and the independent variables was significant. The results of applying these statistcial criteria on the data set, showed that only analysis nos. 2, 3, 7 and 17 in Table 4 were statistically significant and thus suitable for further examination.

From Table 4, the following equations for determination of $c(670)$ then appears:

$$c(670)\ (\mathrm{m}^{-1}) = 1.70\bar{x}\ (\Phi) - 2.80, \quad r^2 = 0.65 \quad (4)$$

$$c(670)\ (\mathrm{m}^{-1}) = 4.28\sigma\ (\Phi) - 2.72, \quad r^2 = 0.46 \quad (5)$$

$$c(670)\ (\mathrm{m}^{-1}) = 0.15\mathrm{SSC}\ (\mathrm{mg/l}) - 4.02\sigma\ (\Phi) - 4.26, \quad r^2 = 0.75 \quad (6)$$

$$c(670)\ (\mathrm{m}^{-1}) = 0.14\mathrm{SSC}\ (\mathrm{mg/l}) + 5.45\sigma\ (\Phi) + 0.16\mathrm{VC}\ (\mu\mathrm{l/l}) - 8.78,$$
$$r^2 = 0.85 \quad (7)$$

It appears, that when using a one-variable model, the variation in $c(670)$ is best explained by the variation in $\bar{x}$ (Eq. (4)). This is most likely partly explained by the fairly narrow variation in SSC. When using a two-variable model, the variation in $c(670)$ is explained by the SSC and the variation in σ (Eq. (6)). When using a three-variable model, the variation in $c(670)$ is explained by the variation in SSC, σ and VC (Eq. (7)). If one wanted to use the LISST-100 measurements to determine SSC, Eqs. (6) and (7) would be useable. An equation containing $\bar{x}$, SSC and ND would be more desirable and probably more robust. However, the limitation of the present dataset does not warrant such an equation. It is noteworthy, that the single parameters best correlated with c is $\bar{x}$ and σ and not SSC (Eqs. (4) and (5)). This emphasises the need for measuring more than one parameter when trying to correlate optical measurements with SSC. It is also remarkable, that even though the regression analysis is based on a small number of samples, the parameters in the regression equations do not change randomly, when the number of variables is increased. That is, in Eq. (5), σ is significant in explaining the variation in $c(670)$. Adding one more parameter (Eq. (6)), it is seen, that σ is still incorporated in the regression, now together with SSC. Adding a third parameter (Eq. (7)), σ and SSC together with VC now determines the variation in $c(670)$.

It is quite clear from Table 4, Fig. 7 and Eqs. (6) and (7), that the accuracy with which SSC can be determined increases, when not only the beam attenuation coefficient is used in the regression analyses, but also parameters describing the quality of the suspended sediment, in this case σ and VC. This has consequences when using in situ calibrations of transmissometers to calculate, e.g. sediment fluxes, where one certainly must consider the probability for changes in in situ particle size during the deployment period. Consequently, LISST measurements can be used to improve, e.g. sediment flux calculations based on optical measurements.

3.5. Theoretical difference in settling velocities

From Table 1, the mean value of $\bar{x}$ in profile I and IV is found to 4.7 (39 μm) and 3.7 Φ (77 μm), respectively. From Table 2, the effective density in profile I and IV is found to 1136 and 490 kg/m^3, respectively. From these values, the theoretical ratio of the settling velocities between the two profiles can be calculated according to the Stokes Law Eq. (8)

$$W_s = \frac{d^2(\rho_F - \rho_W)g}{18 \times \mu} \quad (8)$$

where W_s is the settling velocity, d the diameter of the particle settling and μ the molecular viscosity.

According to Eq. (8), the ratio between two settling velocities, W_{s_1} and W_{s_2}, in the same body of water (where μ and g can be considered constant) is related to the ratio between d and $(\rho_F - \rho_W)$:

$$\frac{W_{s_1}}{W_{s_2}} = \left(\frac{d_1}{d_2}\right)^2 \times \frac{(\rho_F - \rho_W)_1}{(\rho_F - \rho_W)_2} \quad (9)$$

Between profile I and IV, the mean diameter increases approximately by a factor of 2, while the effective density decreases by a factor of 2.3. Substituting these values in Eq. (9) yields Eq. (10)

$$\frac{W_{s_I}}{W_{s_{IV}}} = 2^2 \times \frac{1}{2.3} = \frac{4}{2.3} = 1.7 \quad (10)$$

It is then seen from Eq. (10), that the ratio between settling velocities one should expect to observe between profile I and IV is in the order of a factor 1.7. As the accuracy with which settling velocities from settling tube experiments can be determined usually is in the order of ±20% (Pejrup and Edelvang, 1996), there should be no large differences in in situ settling velocities within the plume when measured with, e.g. the common Braystoke SK110 settling tube, described by Pejrup (1988). This actually is in accordance with settling tube measurements carried out in dredging plumes similar to the one described in this study (Edelvang, 1998), where the in situ settling velocity was found to be almost constant throughout the plume. As it has been rendered probable that an almost constant in situ settling velocity can be found, even though the in situ particle size

changes, this means that settling tube measurements may be poor indicators of flocculation.

3.6. Time-scale of flocculation

When carrying out the profiling sessions within the plume, the research vessel drifted freely within the current. At one point (not shown in Fig. 1) the research vessel drifted for 15 min, while the position was logged. During the 15 min, the research vessel drifted 420 m, yielding an average drift velocity of 0.48 m/s. Consequently it is assumed in the following that the current velocity was 0.48 m/s (this velocity considered a mean water body velocity). This method, although somewhat crude, is considered justifiable, as a current velocity of 0.48 m/s is not uncommon in the Øresund and as the wind velocity was low this day.

The distance between profile I and profile III is approximately 1500 m. This corresponds to a travel time of approximately 50 min. As it appears from Fig. 3 that aggregation took place mainly between profile I and III it can be concluded that the flocculation observed took place within a time-scale of 50 min.

To the knowledge of the authors, no other in situ flocculation time exists in the literature for comparison. Milligan (1995) carried out a mesocosm experiment simulating slack water conditions and found that the suspended sediments (originating from the Elbe estuary) apparently flocculated and settled within a time-scale of 10–15 min. Considering that the results presented here were obtained in a natural environment, with lime sediments known not to possess any electrical charge, there seems to be some agreement between the two studies. Gonzalez and Hill (1998) estimated a flocculation time of approximately 14 days at a mass concentration of 10 mg/l. However, their model was set up for deep-sea conditions not applicable to the near coastal waters investigated in this study with their, in general, higher values of turbulence intensity and SSC.

Recently, Winterwerp (1999) has modelled flocculation times as a function of SSC, turbulence, height above the bed, current velocity, grain-size of the primary particles and the fractal dimension of the suspended particles. He found that the flocculation time could be of the order of minutes to hours. For example, flocculation times in the order of 1–3 min were reported for particles with a primary particle diameter of 4 μm and SSC at 1200 mg/l. With a primary particle diameter of 9 μm and a SSC of 15 mg/l as representative for the data presented in this paper, a flocculation time of approximately one and a half hour would be the result. This is in quite good accordance with the flocculation time of 50 min suggested earlier in this section and is considered satisfactorily, as the model results reported by Winterwerp (1999) showed that flocculation time could vary by two orders of magnitude.

4. Conclusions

Measurements in four profiles with a LISST-100 in situ laser in a lime dredging plume between Denmark and Sweden showed the following.

The suspended sediment, with a concentration range of 7–24 mg/l, was found to change its in situ size spectra from a relatively fine-grained, poorly sorted distribution ($\bar{x} = 4.6\ \Phi$ (41 μm); $\sigma = 1.7\ \Phi$) to a coarser-grained, better sorted distribution ($\bar{x} = 3.2\ \Phi$ (109 μm); $\sigma = 1.4\ \Phi$) over a distance of 1.5 km. The grain-size distribution and the sorting of the primary particles did not change ($\bar{x}_p = 6.8\ \Phi$ (9 μm); $\sigma_p = 1.9\ \Phi$), showing that the change in the in situ size spectra was related to flocculation.

It is demonstrated (Eq. (2)), how it is possible to calculate the effective mean density of the suspended particles/aggregates. In this manner it was found that the effective mean density decreased with increasing in situ mean grain-size of the suspended sediment. This also shows that the suspended sediment in the dredging plume flocculated.

The effective mean densities for the fine-grained distributions (profile I and II) were above 1000 kg/m^3, which differs somewhat from measurements using video analysis. This discrepancy can be related to the fact that the video-systems are only capable of measuring sizes larger than 20–50 μm, while the LISST-100 measures flocs as well as the single mineral grains.

A multiple linear correlation was carried out between $c(670)$ and the variables with which it was considered dependent: SSC, VC, $\bar{x}$, σ and ND. It was found, that when using a one-variable model, the variation in $c(670)$ was best explained by $\bar{x}$ (Eq.

(4)). When using a two-variable model, the variation in $c(670)$ was best explained by SSC and σ (Eq. (6)). When using a three-variable model, the variation in $c(670)$ was best explained by SSC, σ and VC (Eq. (7)).

The regression analyses showed that the accuracy with which $c(670)$ can be determined increases when not only SSC is used in the regression analyses, but also parameters describing the quality of the suspended sediment, in this case σ and VC. This should be considered, when using in situ calibrations of transmissometers to calculate, e.g. sediment fluxes, where one certainly should consider the probability for changes in in situ particle size during the deployment period.

By use of Stokes Law, the calculated effective mean densities and the measured in situ mean grain-sizes, it was possible to calculate the theoretical difference in settling velocity between profile I (mainly unflocculated particles) and profile IV (mainly flocculated particles) (Eqs. (9) and (10)). The settling velocity was found to differ approximately a factor of 1.7, even though there was a large difference in in situ grain-size spectra. This was due to the counter-balancing effect of decreasing density with increasing in situ particle size. The difference in settling velocity is in accordance with earlier measurements of settling velocities in similar dredging plumes in the area, where the settling velocity was found to be almost constant. This shows that measurements and comparisons of settling velocities may be poor indicators of flocculation.

The time-scale of flocculation was calculated by use of the distance between the profiles where flocculation is seen to occur (profile I and III) and a rough estimate of the mean current velocity. In this manner, the time-scale of flocculation was found to be in the order of 50 min, which is in quite good accordance with recent modelling work.

Acknowledgements

The LISST-100 measurements were carried out as a part of the DECO-project (Danish Environmental Monitoring of Coastal Waters), financed by grant no. 9600667 from the Danish Space Board, the Danish Natural Science Research Council, the Danish Technical Research Council and the Danish Agricultural and Veterinary Research Council. Thanks goes to skipper Björn Becker on RV *Sensor* for good seamanship during the cruise. Morten Holtegaard, Danish Hydraulic Institute/Technical University of Denmark is thanked for assistance during the cruise.

References

Agrawal, Y., Pottsmith, H.C., 1994. Laser diffraction particle sizing in STRESS. Cont. Shelf Res. 14, 1101–1121.

Agrawal, Y.C., McCave, I.N., Riley, J.B., 1991. Laser diffraction size analysis. In: Syvitski, J.P.M. (Ed.). Principles, Methods, and Application of Particle Size Analysis. Cambridge University Press, Cambridge, pp. 119–128.

Agrawal, Y., Pottsmith, H.C., Lynch, J., Irish, J., 1996. Laser instruments for particle size and settling velocity measurements in the coastal zone. Proc. IEEE Ocean. Engineer. Soc., 1135–1142.

Amos, C.L., Grant, J., Daborn, G.R., Black, K., 1992. Sea carousel — a benthic, annular flume. Estuar. Coast. Shelf Sci. 34, 557–577.

Baker, E.T., Lavelle, J.W., 1984. The effect of particle size on the light attenuation coefficient of natural suspensions. J. Geophys. Res. 89, 8197–8203.

Bale, A.J., 1996. In situ laser optical particle sizing. J. Sea Res. 36, 31–36.

Bale, A.J., Morris, A.W., 1987. In situ measurement of particle size in estuarine waters. Estuar. Coast. Shelf Sci. 24, 253–263.

Benns, E.J., Pilgrim, D.A., 1994. The effect of particle characteristics on the beam attenuation coefficient and output from an optical backscatter sensor. Neth. J. Aquat. Ecol. 28, 245–248.

Biggs, C.A., Lant, P.A., 2000. Activated sludge flocculation: on-line determination of floc size and the effect of shear. Water Res. 34, 2542–2550.

Campbell, D.E., Spinrad, R.W., 1987. The relationship between light attenuation and particle characteristics in a turbid estuary. Estuar. Coast. Shelf Sci. 25, 53–65.

Conner, C.S., De Visser, A.M., 1992. A laboratory investigation of particle size effects on an optical backscatterance sensor. Mar. Geol. 108, 151–159.

Drake, D.E., 1974. Distribution and transport of suspended particulate matter in submarine canyons off Southern California. In: Gibbs, R.J. (Ed.). Suspended Solids in Water. Plenum Press, New York, pp. 133–153.

Edelvang, K., 1998. In situ settling velocities and concentrations of suspended sediment in spill plumes, Øresund, Denmark. In: Vollmer, M., Grann, H. (Eds.). Large-scale Constructions in Coastal Environments. Springer, Berlin, pp. 181–189.

Eisma, D., 1993. Suspended Matter in the Aquatic Environment. Springer, Berlin, 315pp.

Fennessy, M.J., Dyer, K.R., Huntley, D.A., 1994. INSSEV: an instrument to measure the size and settling velocity of flocs in situ. Mar. Geol. 117, 107–117.

Gardner, W.D., Biscaye, P.E., Zaneveld, J.R.V., Richardson, M.J., 1985. Calibration and comparison of the LDGO nephelometer

and the OSU transmissometer of the Nova Scotian rise. Mar. Geol. 66, 323–344.
Gentien, P., Lunven, M., LeHaître, M., Duvent, J.L., 1995. In-situ depth profiling of particle sizes. Deep-Sea Res. I 42, 1297–1312.
Gibbs, R.J. (Ed.), 1974. Suspended Solids in Water. Plenum Press, New York, 320pp.
Gibbs, R.J., 1982. Floc stability during Coulter–Counter size analysis. J. Sediment. Petrol. 52, 657–660.
Gibbs, R.J., 1985. Estuarine flocs: their size, settling velocity and density. J. Geophys. Res. 90, 3249–3251.
Gibbs, R.J., Wolanski, E., 1992. The effect of flocs on optical backscattering measurements of suspended material concentration. Mar. Geol. 107, 289–291.
Gippel, C.J., 1989. The use of Turbidity Instruments to Measure Stream Water Suspended Sediment Concentration. Monograph Series No. 4. Department of Geography and Oceanography, University College, Australian Defence Force Academy, Canberra, 204pp.
Gonzalez, E.A., Hill, P.S., 1998. A method for estimating the flocculation time of monodispersed sediment suspensions. Deep-Sea Res. I 45, 1931–1954.
Jago, C., Jones, S.E., 1998. Observation and modelling of the dynamics of benthic fluff resuspended from a sandy bed in the southern North Sea. Cont. Shelf Res. 18, 1255–1282.
Jones, D., Wills, M.S., 1956. The attenuation of light in sea and estuarine water in relation to the concentration of suspended solid matter. J. Mar. Biol. Assoc. UK 35, 431–444.
Kranck, K., 1975. Sediment deposition from flocculated suspensions. Sedimentology 22, 111–123.
Kranck, K., 1981. Particulate matter grain-size characteristics and flocculation in a partially mixed estuary. Sedimentology 28, 107–114.
Lick, W., Huang, H., Jepsen, R., 1993. Flocculation of fine-grained sediments due to differential settling. J. Geophys. Res. 98, 10279–10288.
McCabe, J.C., Dyer, K.R., Huntley, D.A., Bale, A.J., 1993. The variation of floc sizes within a turbidity maximum at spring and neap tides. Coast. Engineer. 3, 3178–3188.
McCave, I.N., 1983. Particulate size spectra, behaviour, and origin of nepheloid layers over the Nova Scotian continental rise. J. Geophys. Res. 88, 7647–7666.
Mikkelsen, O., Pejrup, M., 1998. Comparison of flocculated and dispersed suspended sediment in the Dollard estuary. Sedimentary Processes in the Intertidal Zone, Black, K.S., Paterson, D.M., Cramp, A. (Eds.). Geol. Soc. Lond. Spec. Publ. 139, 199–209.
Milligan, T.G., 1995. An examination of the settling behaviour of a flocculated suspension. Neth. J. Sea Res. 33, 163–171.
Pejrup, M., 1988. Flocculated suspended sediment in a micro-tidal environment. Sediment. Geol. 57, 249–256.
Pejrup, M., Edelvang, K., 1996. Measurements of in situ settling velocities in the Elbe estuary. J. Sea Res. 36, 109–113.
Riethmüller, R., Fanger, H.-U., Grabemann, I., Krasemann, H.L., Ohm, K., Böning, J., Neumann, L.J.R., Lang, G., Markofsky, M., Schubert, R., 1988. Hydrographic measurements in the turbidity zone of the Weser Estuary. In: Dronkers, J., van Leussen, W. (Eds.). Physical Processes in Estuaries. Springer, Berlin, pp. 332–344.
Spinrad, R.W., Zaneveld, J.R.V., Kitchen, J.C., 1983. A study of the optical characteristics of the suspended particles in the benthic nepheloid layer of the Scotian rise. J. Geophys. Res. 88, 7641–7645.
Ten Brinke, W.B.M., 1994. In situ aggregate size and settling velocity in the Oosterschelde tidal basin (the Netherlands). Neth. J. Sea Res. 32, 23–35.
Traykovski, P., Latter, R.J., Irish, J.D., 1999. A laboratory evaluation of the laser in situ scattering and transmissometery instrument using natural sediments. Mar. Geol. 159, 355–367.
Tsai, C.-H., Iacobellis, S., Lick, W., 1987. Flocculation of fine-grained lake sediments due to a uniform shear stress. J. Great Lakes Res. 13, 135–146.
Van der Lee, W.T.B., 1998. The impact of fluid shear and the suspended sediment concentration on the mud floc size variation in the Dollard estuary, The Netherlands. Sedimentary processes in the intertidal zone, Black, K.S., Paterson, D.M., Cramp, A. (Eds.). Geol. Soc. Lond. Spec. Publ. 139, 187–198.
Van Leussen, W., 1994. Estuarine macroflocs and their role in fine-grained sediment transport. PhD thesis, University of Utrecht, 488pp.
Wells, J.T., Kim, S.-Y., 1991. The relationship between beam transmission and concentration of suspended particulate material in the Neuse river estuary, North Carolina. Estuaries 14, 395–403.
Winterwerp, J.C., 1999. On the dynamics of high-concentrated mud suspensions. PhD thesis, Technical University of Delft, 172pp.